

Scanning Ion Conductance Microscopy of Living Cells

Yuri E. Korchev,* C. Lindsay Bashford,# Mihailo Milovanovic,# Igor Vodyanoy,*[§] and Max J. Lab*

*Department of Physiology, Charing Cross and Westminster Medical School, University of London, London W6 8RP; #Division of Biochemistry, St. George's Hospital Medical School, University of London, London SW17 0RE; and [§]Office of Naval Research Europe, London NW1 5TH, England

ABSTRACT Currently there is a great interest in using scanning probe microscopy to study living cells. However, in most cases the contact the probe makes with the soft surface of the cell deforms or damages it. Here we report a scanning ion conductance microscope specially developed for imaging living cells. A key feature of the instrument is its scanning algorithm, which maintains the working distance between the probe and the sample such that they do not make direct physical contact with each other. Numerical simulation of the probe/sample interaction, which closely matches the experimental observations, provides the optimum working distance. The microscope scans highly convoluted surface structures without damaging them and reveals the true topography of cell surfaces. The images resemble those produced by scanning electron microscopy, with the significant difference that the cells remain viable and active. The instrument can monitor small-scale dynamics of cell surfaces as well as whole-cell movement.

INTRODUCTION

The cell membrane, a multifunctional and dynamic structure, is an absolute condition for life. Yet techniques for real-time investigation of the membrane functions of intact cells are limited. We have developed an instrument for studying both the topography and certain functional properties of the surface of living cells. The instrument combines elements from a conventional patch-clamp apparatus used in electrophysiological studies of cell membranes (Hille, 1992) with those of scanning probe microscopy (SPM) (Hansma et al., 1989; Binnig and Rohrer, 1982; Binnig et al., 1986; Bard et al., 1991). In SPM, an appropriately designed sensitive tip scans the surface of a sample, close enough to detect specific physical/chemical surface characteristics and its relief. The tip's output is used to generate a map of the chosen characteristic of the scanned surface.

There is a great interest in applying SPM to the imaging of biological macromolecules, cellular organelles, and cells (Driscoll et al., 1990; Arkawa et al., 1992; Radmacher et al., 1992; Henderson et al., 1992; Hansma and Hoh, 1994; Lal and John, 1994). However, the interaction between the microscope's tip and the sample remains only partially understood. Consequently, the soft surface of the sample is often damaged during imaging (Schoenenberger and Hoh, 1994; Hansma and Hoh, 1994; Lal and John, 1994). In atomic force microscopy (AFM), the "tapping in liquid" mode of operation (Putman et al., 1994) has greatly reduced the damage. Nevertheless, the mechanism(s) of image generation and their interpretation are unclear, and the nature of

the adhesive interaction between the AFM tip and a "sticky" specimen remains problematical.

Hansma et al. (1989) demonstrated a scanning ion-conductance microscope that utilizes a glass micropipette as the scanning probe. The fragile micropipettes often broke on contact with the sample or during high-speed scans, thus limiting their usefulness. Microfabrication of more robust silicon probes improved matters to some extent, and allowed faster scanning (Prater et al., 1991). Recently, the same group has developed a "tapping mode" SPM (Proksch et al., 1996) in which a bent micropipette is used both as a cantilever and as a current-sensitive probe. However, all of their applications were limited to the imaging of flat polymeric films.

PRINCIPLE OF OPERATION

To scan living cells without damaging them or the micropipette tip, we have developed a specific scanning protocol that prevents the tip of the micropipette from making direct physical contact with the specimen. The position of the tip relative to the sample surface strongly influences the ion current (I) through the pipette, which provides the feedback signal to control the vertical position of the tip. This ion current depends on the overall resistance of the tip (Fig. 1), which is the combination of the resistance (R_p) of the micropipette itself and the access resistance (R_{Ac}) of the micropipette opening. Pipette resistance can be easily calculated as the resistance of the electrolyte inside the pipette tip, where the pipette tip can be considered as the frustum of a right circular cone, with a base radius that of the glass tube from which the pipette was pulled, an apex radius (r) that of the pipette opening, and height that of the micropipette tip filled with electrolyte. Access resistance is defined as resistance along the convergent paths from the bath to the micropipette opening. It is often used by electrophysiologists who study ionic channels (Hille, 1992; Hall, 1975;

Received for publication 6 February 1997 and in final form 21 April 1997.

Address reprint requests to Dr. Yuri E. Korchev, Department of Physiology, Charing Cross and Westminster Medical School, Fulham Palace Road, London W6 8RF, England. Tel.: 44-181-846-7643; Fax: 44-181-846-7338; E-mail: y.korchev@cxwms.ac.uk.

© 1997 by the Biophysical Society

0006-3495/97/08/653/06 \$2.00

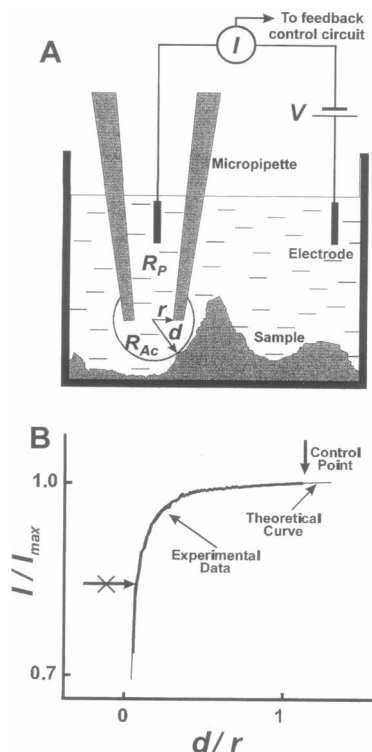


FIGURE 1 Diagram of sensing mechanism of the scanning ion conductance microscope. (A) The micropipette tip/surface interaction. The position of the micropipette tip relative to the sample surface strongly influences the access resistance (R_{Ac}) and, consequently, the ion current (I) flowing through the pipette. The current value at a distance (d) that exceeds the radius (r) can be used to control the vertical position of the tip to sense neighboring structures that are higher than the vertical sample/probe separation. During the scan, the tip of the pipette, with its "spherical current sensor" of radius d , "rolls" over surface irregularities of the specimen without damaging it. (B) Comparison of expected and actual values of tip current (I) as a function of the sample/tip separation (d). The theoretical curve was calculated for a simplified model of a frustum (truncated cone)-shaped tip of known geometry approaching a flat, nonconductive surface. The experimental data show the approach characteristic of a tip of similar geometry. The vertical arrow indicates the value of current (control point) used for the scanning protocol in the feedback control circuit.

Vodyanoy and Bezrukov, 1992). Generally, R_{Ac} is a complex function of the distance (d) between the sample and the probe, and the geometry and electrochemical properties of the sample surface. The current (I) through the pipette, which is measured directly, is given by

$$I = \frac{V}{R_p + R_{Ac}(d)} \quad (1)$$

where V is the voltage applied to the electrodes. Equation 1 can be solved numerically for a simple model of the tip approaching a flat, nonconductive surface. Fig. 1 B illustrates the good agreement between the experimental data and the theoretical curve calculated for a pipette geometry similar to that used to obtain the experimental curve. The vertical axis represents the normalized current (I_{max} is the

current when the tip is far from the surface). The horizontal axis is the sample/tip separation distance expressed in r . The crossed arrow indicates the region where the position of the probe relative to the local sample surface strongly influences the measured ion current. When this is used as the set-point current for the feedback loop, it will control the vertical position of the tip with maximum sensitivity. However, the tip of the probe is very close to the sample, and therefore has limited sensitivity toward neighboring structures that are higher than the sample/tip separation. During a scan with this set point, the tip of the pipette will then break, damage the specimen, or both. To overcome this problem it is important to move the set-point current of the feedback loop to a value observed when the distance d exceeds that of r (Fig. 1). This produces effectively a "spherical sensor" of diameter d that can "roll" over surface irregularities in the specimen without damaging it or the pipette tip.

EXPERIMENTAL SET-UP

The present instrument is based on an inverted optical microscope (Diaphot 200; Nikon Corporation, Tokyo, Japan) with a mechanism for coordinating optical and scanned images, using a video camera with "frame-grabbing" hardware and software. It consists of a computer-controlled three-axis translation stage with measurement and feedback systems (East Coast Scientific, Cambridge, England), which scans the micropipette tip over the specimen. For living cells, displacements in excess of 30–50 μm in the vertical direction are required. We have therefore used a three-axis piezotranslation stage (Triton; Piezosystem, Jena, Germany) with a 100- μm travel distance in the x , y , and z directions.

The micropipettes were made from 1.00-mm outer diameter, 0.78-mm inner diameter glass microcapillaries on a laser-based Brown-Flaming puller (model P-2000; Sutter Instrument Company, San Rafael, CA) with constant outer/inner diameter ratios along their entire lengths and a defined tip geometry (Brown and Flaming, 1986). We estimated the tip radius of the micropipettes used in the present series of experiments to be ~ 25 nm, and the cone angle of the tip to be $\sim 1.5^\circ$.

The micropipettes and the bath were filled with the same solutions (usually physiological or growth media) to avoid salt concentration gradient cell potentials and liquid junction potentials. Ag/AgCl electrodes, in the bath and pipette, provided an electrical connection in a conventional electrophysiological circuit. The ion currents flowing into the pipette were measured at applied DC voltages of 50–200 mV and were used in the feedback loop that controlled the micropipette's vertical position (Fig. 1 A). The lateral image resolution was usually 512×512 or 1024×1024 pixels with 16-bit vertical resolution. Typically, a single scan takes several minutes to acquire. However, the imaging of a large area of the highly elaborated surface can last up to 10 min. The samples were usually placed on petri dishes and

FIGURE 2 Scanning ion-conductance microscope images of murine melanocyte line melan-b. The cells were grown as previously described (Bennett et al., 1989). The melan-b cells tend to be bipolar and aligned with each other. Raised nuclear areas of cells are visible (*A*, bright highlights in *B* and *C*). Cell borders commonly show processes (dendrites) formed by melanocytes. In contrast with epithelial cells, adjacent cells appear largely nonadherent, but with localized contacts. Images *B* and *C* were selected from a longer sequence of successive scans. Each scan took less than 5 min to acquire, and image *C* was obtained at higher magnification.

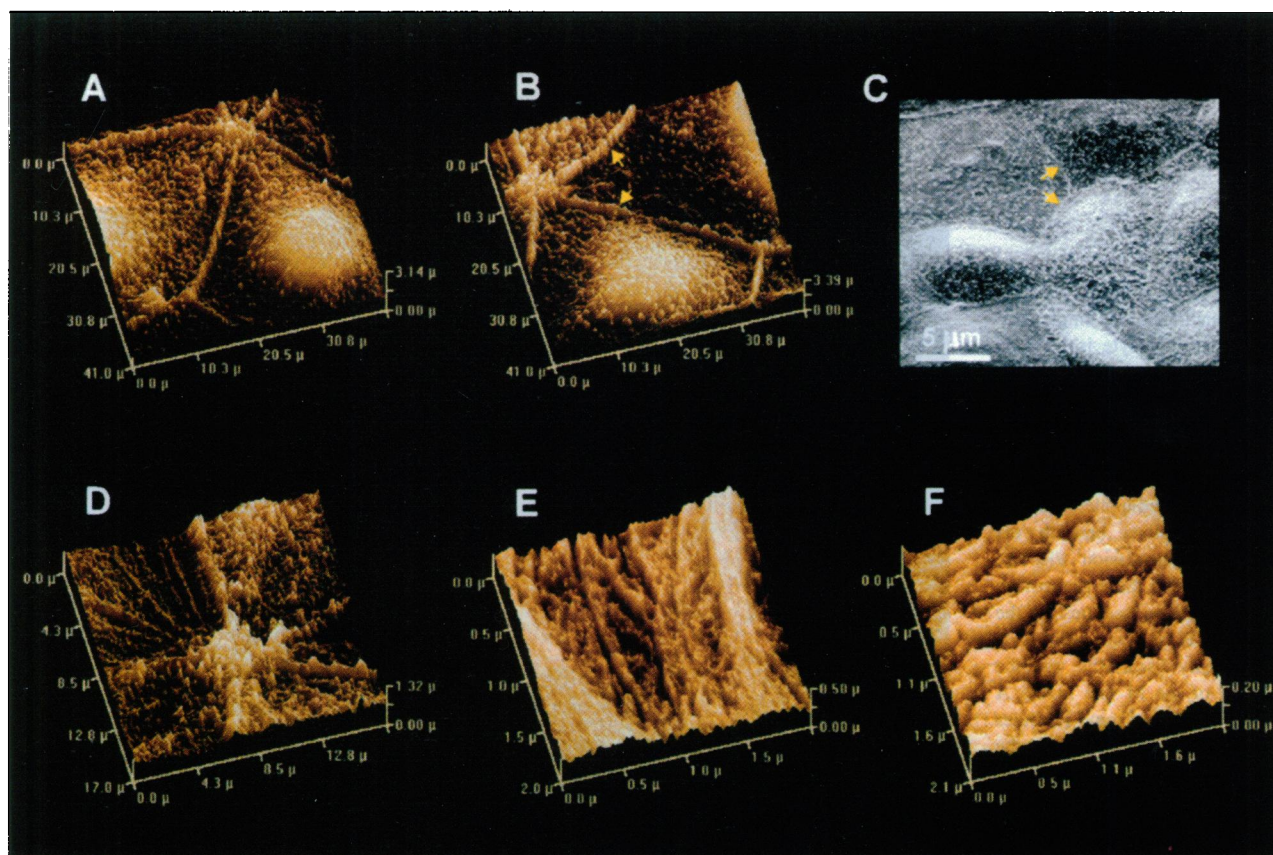
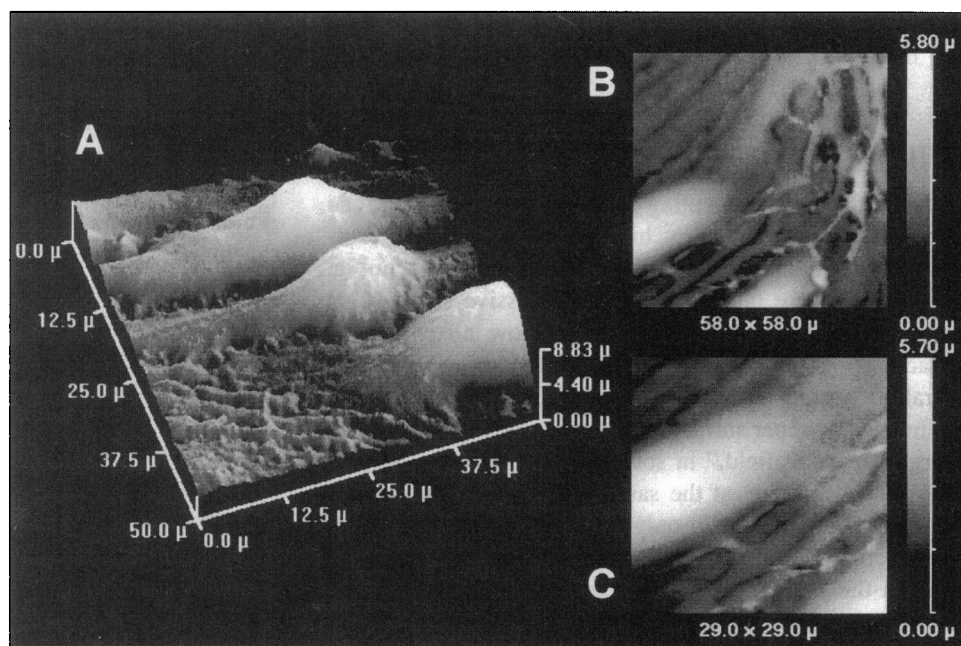


FIGURE 3 (*A, B, D–F*) Scanning ion-conductance microscope images, in real time, of a confluent monolayer of a human colon cancer cell line (Caco-2) in a 1:1 mixture of phosphate-buffered saline and medium (RPMI 1640 with 20% fetal calf serum). During the 8-h period of continuous scanning (monitoring), the cells remain viable and motile. *A* and *B*, separated by 140 min, show movement of the “junction” between five cells. The nuclear regions of two cells are discernible under the membrane as the lighter areas, and the boundaries between cells (*arrows*) appear to be raised. At higher magnification a variety of surface morphologies were observed in the five adjacent cells (*D–F*). One cell (*top left in D*, and at higher magnification, *E*) showed filamentous structures, reminiscent of microfilaments, converging on the “junction.” Other cells had numerous surface projections, possibly microvilli. The projections (*top right in D*, and at higher magnification, *F*) can represent a developing brush border. (*C*) Scanning electron micrograph of Rama 25 mammary carcinoma cells in culture. The cells were grown on plastic in culture medium with serum (Bennett et al., 1978). Microvillous cell surfaces, with denser microvilli marking cell boundaries (*arrows*), can be observed. These cells grow in culture as a single layer (monolayer), similar to the human colon cancer cells. (This scanning electron micrograph was kindly provided by Dr. D. C. Bennett.)

imaged in appropriate medium without any special fixation or treatment.

RESULTS AND DISCUSSION

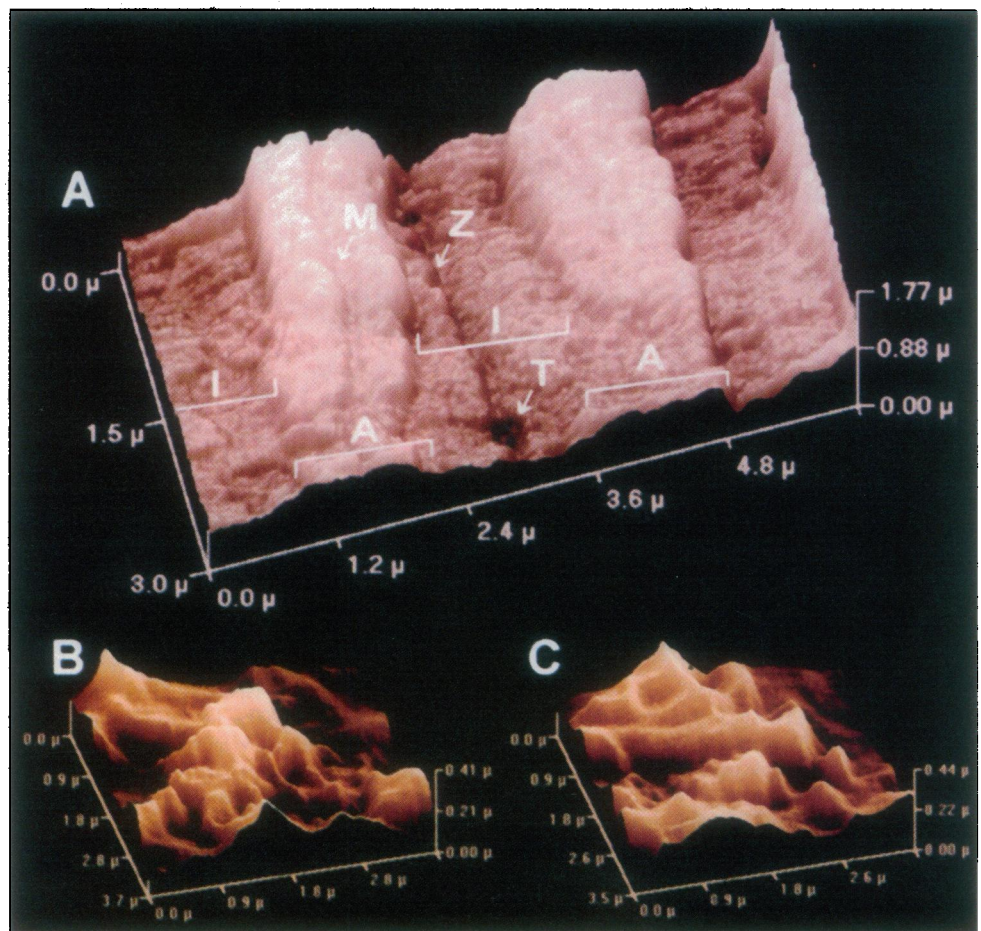
With the developed scanning protocol our instrument can successfully image complex, highly elaborated cellular surfaces without damaging them (Fig. 2). Images shown in Fig. 2, *B* and *C*, were obtained in two successive scans (*C* at higher magnification). These images show no change in surface topography that could be related to any possible alteration caused by the scanning probe. The microscope can image the upper surface of the cell in a single scan with a large "depth of field," in some cases better than 30 μm . Importantly, we can, at the same time, detect fine surface structures that are usually only observed by scanning electron microscopy after fixation and staining. Comparison between the scanning electron micrograph (Fig. 3 *C*) and our microscope images (Fig. 3, *A*, *B*, and *D*) of similar epithelial cancer cell lines shows matching cellular morphologies: microvillous cell surfaces with denser microvilli marking cell boundaries (*arrows*). This confirms our contention that images captured by our microscope resemble those obtained by scanning electron microscopy of fixed

and coated material, the significant difference being that in our system, the cells remain viable and active.

As the instrument can scan cells consistently and reproducibly for many hours, we can investigate real-time changes in cell surfaces. Tracking the junctional boundary between five cells from a sequence of images (e.g., Fig. 3, *A* and *B*) over an 8-h period of continuous scanning shows that human colon cancer cells remain motile and thus viable. The addition of cytochalasin B, a compound that inhibits actin polymerization, abolishes the movement. We suggest that the filamentous structures apparent in Fig. 3 (*D* and *E*) can be membrane manifestations of a cytoskeletal regulator of cell movement. At higher magnification, the smaller filamentous structures appear as furrows (Fig. 3 *E*) that can reflect an interaction between internal microfilaments and the cell membrane. This observation is important because it contrasts with AFM studies of the cell surface. In AFM images the microfilamentous structures are directed upward, probably as a result of tip-induced deformation of the cell plasma membrane around the microtubules (Henderson et al., 1992; Hansma and Hoh, 1994; Lal and John, 1994); valleys or depressions are poorly resolved.

Confluent human colon cancer cells (Caco-2) are known to undergo enterocytic differentiation in culture (Rousset,

FIGURE 4 (A) Surface topography of a small area of a single, quiescent cardiac myocyte isolated by digestion of intact perfused ventricle. The surface structure is comparable to that observed by scanning and transmission electron microscopy (Sommer and Jennings, 1991). The main contractile elements appear as protrusions beneath the membrane. Transmission electron microscopy shows these protrusions in cross section as "scallops" in the sarcolemma. Bands equivalent to A and I are easily discernible, with the suggestion of the M line in the A band. The opening of some T tubules (T) are visible in what would be the Z-line groove. (*B* and *C*) Topographical images (scanned 1 min apart, taking 2 min each) of isolated smooth muscle cell illustrating the movements of the cell surface in Ca^{2+} -containing medium (2.5 mM). The experiment was performed at room temperature on single guinea pig ileal smooth muscle cells obtained after collagenase treatment, as described elsewhere (Zholos et al., 1994).



1986). The highly developed microfilamentous structures suggest that such differentiation processes can have occurred at the time of observation. Usually, Caco-2 cells spread over the surface during growth and organize as a cell monolayer. Fig. 3 shows numerous surface projections, possibly microvilli (e.g., Fig. 3 *D*, top right cell). Dense microvilli in Fig. 3, *A*, *B*, *C*, and *E* (marked by arrows in *B* and *C*) can indicate where neighboring cells make contact and form "tight" junctions. The projection shown in Fig. 3 *F* can indicate a developing brush border as a part of enterocytic differentiation of confluent Caco-2 cells in culture (Rousset, 1986).

One significant aspect of our instrument, in contrast with other SPMs, is that it is possible to scan the entire surface (upper and lower) of an isolated cell, provided that the cell does not adhere to its substrate. We can use the microscope probe to mechanically manipulate the cell to expose the surfaces of interest to a position accessible for scanning. Fig. 4 *A* presents the surface topography of an isolated quiescent cardiac myocyte. The surface structures visualized with our apparatus can be analogous to the "scallop" of the membrane seen in conventional electron micrographs (Sommer and Jennings, 1991). Some of the surface structures can represent the membrane projections of the contractile apparatus (possibly A and I bands, M lines or H zones in the A band, the openings of some T tubules (T) that appear to be in the Z line groove). The dimensions we observe are consistent with those found in electron micrographs of cardiac myocytes (Sommer and Jennings, 1991).

Importantly, the system follows small changes in cell surfaces in real time. Fig. 4 (*B* and *C*) shows the cell surface of one smooth muscle cell in Ca^{2+} -containing medium. The change in surface relief (compare *A* and *B*) reflects the dynamics of the cell surface. Live smooth muscle cells in Ca^{2+} -free solution or dead cells demonstrate no such surface dynamics. Previous studies (Zholos and Bolton, 1994) have shown that the stable muscarinic agonist carbachol, when applied to smooth muscle cells, evokes a large cationic current that oscillates because of regular spike-like increases in cytosolic Ca^{2+} . We found that carbachol radically and rapidly induced changes in the cell surface. The observed correlation between cytosolic Ca^{2+} and cell surface motility could imply cytoskeletal dynamics reflected in the cell surface. Indeed, the addition of cytochalasin B, an inhibitor of actin polymerization, eliminates most of the cell surface movement.

SUMMARY

Our scanning ion conductance microscope produces high-resolution images comparable with those of scanning electron microscopy. It produces 3D images of living cells in real time, with a large depth of field, and can detect the fine dynamic behavior of cell surfaces as well as grosser cellular movements. It can also double as a fully fledged patch-clamp apparatus, and can be used for micromanipulation of

living cells, microsurgery, microinjection, or drug delivery. Further development of the device could include additional cellular imaging with multifunctional probes or other types of real-time microscopy.

We are very grateful to our colleagues at St. George's Hospital Medical School: Dr. D. C. Bennett and Dr. E. V. Sviderskaya (Department of Anatomy and Developmental Biology); Dr. D. J. Winterbourne (Department of Surgery); Prof. T. B. Bolton and Dr. A. V. Zholos (Department of Pharmacology and Clinical Pharmacology) for providing cells, and for advice and support in imaging the living cells. We thank Dr. S. Harding (National Heart and Lung Institute) for providing cardiac cells. We are also very grateful to Prof. C. W. Pitt and Dr. H. Robinson (University College London) and Dr. M. E. Welland (University of Cambridge) for their involvement in the earlier stages of development of the microscope.

Our work is supported by the Garfield Weston Trust, the British Heart Foundation, the Office of Naval Research, the Engineering and Physical Science Research Council, and the Cell Surface Research Fund.

REFERENCES

- Arkawa, H., K. Umemura, and A. Ikai. 1992. Protein images obtained by STM, AFM and TEM. *Nature*. 358:171-173.
- Bard, A. J., F. F. Fan, D. T. Pierce, P. R. Unwin, D. O. Wipf, and F. Zhou. 1991. Chemical imaging of surfaces with the scanning electrochemical microscope. *Science*. 254:68-74.
- Bennett, D. C., P. J. Cooper, T. J. Dexter, L. M. Delvin, J. Heasman, and B. Nester. 1989. Cloned mouse melanocyte lines carrying the germline mutations albino and brown: complementation in culture. *Development*. 105:379-385.
- Bennett, D. C., L. A. Peachey, H. Durbin, and P. S. Rudland. 1978. A possible mammary stem cell line. *Cell*. 15:283-298.
- Binnig, G., C. F. Quate, and C. Gerber. 1986. Atomic force microscope. *Phys. Rev. Lett.* 56:930-933.
- Binnig, G., and H. Rohrer. 1982. Scanning tunnelling microscopy. *Helv. Phys. Acta*. 55:726-735.
- Brown, K. T., and D. G. Flaming. 1986. Advanced Micropipette Techniques for Cell Physiology. Wiley, New York.
- Driscoll, R. J., M. G. Youngquist, and J. D. Baldeschwieler. 1990. Atomic-scale imaging of DNA using scanning tunnelling microscopy. *Nature*. 346:294-296.
- Hall, J. E. 1975. Access resistance of a small circular pore. *J. Gen. Physiol.* 66:531-532.
- Hansma, H. G., and J. H. Hoh. 1994. Biomolecular imaging with the atomic force microscope. *Annu. Rev. Biophys. Struct.* 23:115-139.
- Hansma, P. K., B. Drake, O. Marti, S. A. C. Gould, and C. B. Prater. 1989. The scanning ion-conductance microscope. *Science*. 243:641-643.
- Henderson, E., P. G. Haydon, and D. S. Sakaguchi. 1992. Actin filament dynamics in living glial cells imaged by atomic force microscopy. *Science*. 257:1944-1946.
- Hille, B. 1992. Ionic Channels of Excitable Membranes. Sinauer, Sunderland, MA.
- Lal, R., and S. A. John. 1994. Biological applications of atomic force microscopy. *Am. J. Physiol.* 266:C1-C21.
- Prater, G. B., P. K. Hansma, M. Tortonese, and C. F. Quate. 1991. Improved scanning ion-conductance microscope using microfabricated probes. *Rev. Sci. Instrum.* 62:2634-2638.
- Proksch, R., R. Lai, P. K. Hansma, D. Morse, and G. Stucky. 1996. Imaging the internal and external pore structure of membranes in fluid: tapping mode scanning ion conductance microscopy. *Biophys. J.* 71:2155-2157.

- Putman, C. A. J., K. O. Werf, B. G. Grooth, N. F. Hulst, and J. Greve. 1994. Viscoelasticity of living cells allows high resolution imaging by tapping mode atomic force microscopy. *Biophys. J.* 67:1749–1753.
- Radmacher, M., R. W. Tillmann, M. Fritz, and H. E. Gaub. 1992. From molecules to cells: imaging soft samples with the atomic force microscope. *Science*. 257:1900–1905.
- Rousset, M. 1986. The human colon carcinoma cell lines HT-29 and Caco-2: two in vitro models for the study of intestinal differentiation. *Biochimie*. 68:1035–1040.
- Schoenenberger, C. A., and J. H. Hoh. 1994. Slow cellular dynamics in MDCK and R5 cells monitored by time-lapse atomic force microscopy. *Biophys. J.* 67:929–936.
- Sommer, J. R., and R. B. Jennings. 1991. The Heart and Cardiovascular System. Raven Press, New York. 3–50.
- Vodyanoy, I., and S. M. Bezrukov. 1992. Sizing of an ion pore by access resistance measurements. *Biophys. J.* 62:1–3.
- Zholos, A. V., and T. B. Bolton. 1994. G-protein control of voltage-dependence as well as gating of muscarinic metabotropic channels in guinea-pig ileum. *J. Physiol. (Lond.)*. 478:195–202.
- Zholos, A. V., S. Komori, H. Ohashi, and T. B. Bolton. 1994. Ca^{2+} inhibition of inositol trisphosphate-induced Ca^{2+} release in single smooth muscle cells of guinea-pig small intestine. *J. Physiol. (Lond.)*. 481:97–109.